IMPLICIT LAYERED MOMENT EQUATIONS FOR OPEN CHANNEL FLOW MODELING

Cenling Xia[1] and Yee-Chung Jin[2]

ABSTRACT

Though some 3D models have been emerging and becoming much more powerful than ever for the three dimensional simulation, the well-known depth-averaged models are still very important methods in most open channel flow modeling. However, one of the advantages of the depth-averaged models is that they cannot supply detailed information for the vertical distributions of velocities or pressure.

Multilayer models improve the depth-averaged and moment equations to supply more detailed information while not increasing much computation and complexity. These multilayer models can use explicit or implicit layer dividing method. The governing equations can simply use the basic Reynolds equations in each layer, or the layer averaged equations. Then the simulation is carried out repeatedly from the top layer to the bottom layer until the flow reaches the steady condition. The efficiency of this method is validated by one application case.

KEY WORDS

Multilayer models, depth-averaged, moment equations, layer-dividing method, vertical distribution of velocity.

[1] Sectional lecturer, Faculty of Engineering, University of Regina, 3737 Wascana Parkway, Regina, SK., S4S 0A2, Canada, Phone 306/585-5188, FAX 306/569-7395, Cenlingx@hotmail.com

[2] Professor, Faculty of Engrg., University of Regina, 3737 Wascana Parkway, Regina, SK, S4S 0A2, Canada, Phone 306/585-4567, FAX 306/585-4855, Yee-Chung.Jin@uregina.ca

INTRODUCTION

The depth-averaged models usually can be successfully used for the simulation of open channel flows. The governing equations are obtained by integrating the Reynolds equations over the flow depth based on the assumptions of negligible vertical acceleration, hydrostatic pressure and uniform longitudinal velocity (Chaudhry 1993). These assumptions simplify the computation but limiting the models' capacity to consider more vertical details.

There is no doubt that 3D models have the strongest capacity to extract the information in vertical direction, whereas they need much more computation effects than most depth-averaged models. This disadvantage of 3D models is being overcome with the emergence of more powerful computers.

Besides depth-averaged models and 3D models, there are some other models that can extract information in vertical direction while limiting the added computation of 3D models. Among them are Boussinesq models (Hagger and Hutter 1985; Matthew 1991; Chaudhry 1993), depth-averaged and moment equations (Steffler and Jin 1993), potential flow models (Montes 1995), Dressler curvilinear coordinates models (Dressler 1978; Sivakuaran et al. 1983) and multilayer models (Lai and Yen 1993; Chio 1998; Zarrati and Jin 2004; Lynett and Liu 2004; Xia and Jin 2005*a*, *b*).

In multilayer models, the flow is divided into a series of non-overlapping flow layers, and the simulation of flow is carried out over each layer. Layer dividing can be considered as one way for vertical discretization of the research domain. The governing equations can be the basic Reynolds equations as in most conventional 3D models with structured vertical grids (Lai and Yen 1993), or layer-averaged equations (Chio 1998; Zarrati and Jin 2004; Xia and Jin 2005 *a*, *b*). Layer-averaged equations allow for vertical detailed information while taking advantage of the depth averaged equations of shallow water (Lynett and Liu 2004). Multilayer models can potentially evaluate the velocity and pressure profiles with required accuracy using a proper number of flow layers. They also have high flexibility for complex flow patterns.

GOVERNING EQUATIONS

LAYER DIVIDING

In multilayer models, the layers as shown in figure 1 are non-overlapping, and can be indexed from top to bottom as k =1, …, n. The interfaces are similarly indexed from top to bottom, and the free surface and channel bed are taken as special interfaces, k =0, 1, …, n. The interfaces for layer dividing can be very different in locations and shapes, and they can be carried out by the explicit or implicit methods (Xia and Jin 2005*a*, *b*).

In explicit method, the layer dividing interfaces are determined artificially based on individual experience and the research problems. For example, Reggio (1993) and Wai et al. (1996) used horizontal interfaces. Lai and Yen (1993) forced all layers except the top one to be parallel. The layer-dividing has large randomness and does not account for the flow conditions. In addition, the interface exchanges of mass, energy and moment, make the governing equations much more complicated than classical depth equations.

The implicit method for layer-dividing tries to take into account of the flow conditions and to define the layer interfaces in equation to avoid any randomness,

$$w = \frac{\partial \zeta_k}{\partial t} + u \frac{\partial \zeta_k}{\partial x} \tag{1}$$

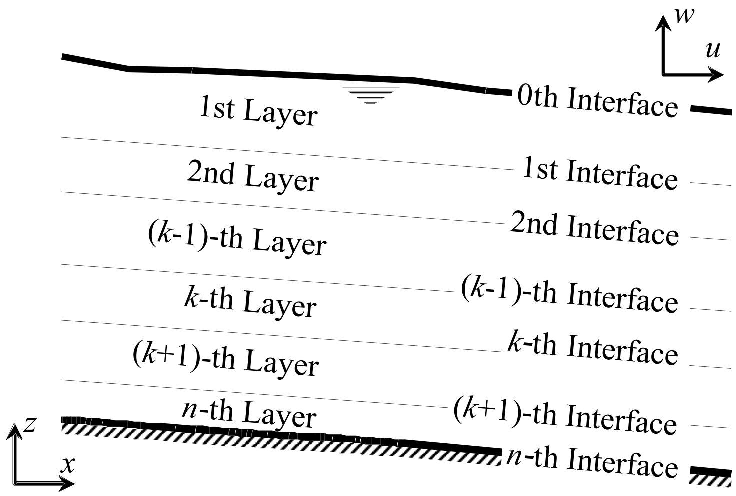

Figure 1: Definition of coordinates and layer index

APPROXIMATE VERTICAL PROFILES OF DEPENDENT VARIABLES

The nodal points are placed along each vertical column. They can be placed at the mid-points of the flow layers or at the interfaces, or both. The number of nodes directly relates to the number of equations available.

The nodes of horizontal velocity are placed at both mid-thickness point and interfaces, and the vertical distribution as in the Figure 2 can be approximated by simply connecting them linearly,

$$u = u_b(1-\eta) + u_s\eta + (2u_c - u_s - u_b)(0.5 - |0.5-\eta|) \tag{2}$$

where u = horizontal velocity; $\eta = (z - z_b)/h$; h = the layer vertical thickness, $h = z_s - z_b$; z = elevation; subscripts "*s*" and "*b*" refer to quantities at the top and bottom surface of the layer, respectively; and subscripts "*c*" refer to quantities at the mid-thickness of the layer.

Another set of coefficients, which may yield a brief form of expressions for equations later, can be defined as,

$$u_0 = (u_s + u_b + 2u_c)/4; \quad u_1 = (u_s - u_b)/2; \quad u_2 = u_c - (u_s + u_b)/2 \tag{3 a, b, c}$$

where subscript "0" represents the vertically averaged quantities of corresponding variables for each layer; subscript "1" represents half of the quantity difference at top and bottom face for each layer; and subscript "2" represents the quantities at the mid-thickness of layer in excess of arithmetic average of upper and lower surfaces.

The nodes of vertical velocity and pressure are placed only at the interfaces and are connected simply using straight-lines. The approximate profiles can be mathematically expressed as (Figure 2),

$$w = w_b(1 - \eta) + w_s\eta \tag{4}$$

$$p = p_b(1 - \eta) + p_s\eta \tag{5}$$

and

$$w_0 = (w_s + w_b)/2; \quad w_1 = (w_s - w_b)/2; \quad w_2 = 0 \tag{6 a, b, c}$$

$$p_0 = (p_s + p_b)/2; \quad p_1 = (p_s - p_b)/2; \quad p_2 = 0 \tag{7 a, b, c}$$

where w = vertical velocity; p = pressure.

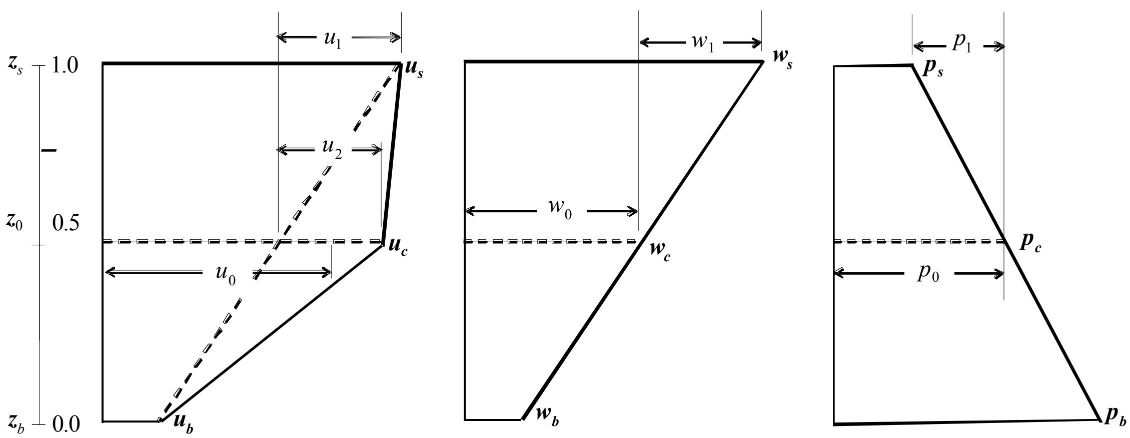

Figure 2: Distribution of velocities and pressure in each layer

LAYER AVERAGED EQUATIONS

Based on the approximate vertical profiles of these parameters, and the requirement of consistence between variables and equations, we obtain the following equations (Xia and Jin 2005*a*, *b*),

Continuity equation

$$\frac{\partial h}{\partial t} + \frac{\partial h u_0}{\partial x} = 0 \tag{8}$$

x-Momentum Equation

$$\frac{\partial h u_0}{\partial t} + \frac{\partial h u_0^2}{\partial x} + \frac{\partial}{\partial x}\left(\frac{1}{3}h u_1^2 + \frac{1}{12}h u_2^2\right) = -\frac{1}{\rho}\frac{\partial h p_0}{\partial x} + \frac{1}{\rho}\left(p_s\frac{\partial z_s}{\partial x} - p_b\frac{\partial z_b}{\partial x}\right) + \frac{1}{\rho}\frac{\partial h\overline{\sigma_x}}{\partial x} + \frac{1}{\rho}\left(F_{xs} - F_{xb}\right) \tag{9}$$

x-Moment Equation

$$\frac{\partial hu_1}{\partial t}+\frac{\partial hu_0u_1}{\partial x}+\left(2u_1^2+\frac{1}{2}u_2^2\right)\frac{\partial z_0}{\partial x}-\frac{1}{2}u_2\frac{\partial}{\partial x}hu_1-\frac{1}{2}u_1\frac{\partial}{\partial x}hu_2-2u_1w_1 = \frac{1}{\rho}\left[6\overline{\sigma}_x\frac{\partial z_0}{\partial x}-6\overline{\tau_{xz}}+3\left(F_{xs}+F_{xb}\right)\right] \tag{10}$$

z-Momentum Equation

$$\frac{\partial hw_0}{\partial t}+\frac{\partial hu_0w_0}{\partial x}+\frac{\partial}{\partial x}\left(\frac{1}{4}hu_1w_1\right) = -\frac{1}{\rho}\frac{\partial h\overline{\tau_{xx}}}{\partial x}-\frac{1}{\rho}\left(p_s-p_b\right)-gh+\frac{1}{\rho}\left(F_{zs}-F_{zb}\right) \tag{11}$$

where x = horizontal coordinate; t = time; g = gravitational acceleration; ρ= the fluid density. F_x and F_z are two composite terms of stresses at interfaces,

$$F_{xs}=\tau_{xzs}-\sigma_{xs}\frac{\partial z_s}{\partial x};\quad F_{xb}=\tau_{xzb}-\sigma_{xb}\frac{\partial z_b}{\partial x} \tag{12a, b}$$

$$F_{zs}=\tau_{xzs}\frac{\partial z_s}{\partial x}-\sigma_{zs};\quad F_{zb}=\tau_{xzb}\frac{\partial z_b}{\partial x}-\sigma_{zb} \tag{13 a, b}$$

where τ_{xz} = τ_{zx} = sheer stress, the first subscript refers to the normal direction of the acting face, the second subscript refers to the direction of acting force ; σ_x and σ_z = normal stresses, the subscript refers to the direction of acting force.

The vertically averaged stresses of each layer are evaluated based on Boussinesq's turbulent stress formula (Versteeg and Malalasekera 1995),

$$\overline{\sigma_x}=\overline{\tau_{xx}}=\frac{1}{h}\int_{z_b}^{z_b+h}\tau_{xx}\,dz=2\rho\nu_t\frac{\partial u_0}{\partial x} \tag{14}$$

$$\overline{\sigma_z}=\overline{\tau_{zz}}=\frac{1}{h}\int_{z_b}^{z_b+h}\tau_{zz}dz=2\rho\nu_t\frac{w_s-w_b}{h} \tag{15}$$

$$\overline{\tau_{xz}}=\overline{\tau_{zx}}=\frac{1}{h}\int_{z_b}^{z_b+h}\tau_{xz}dz=\rho\nu_t\left(\frac{u_s-u_b}{h}+\frac{\partial w_0}{\partial x}\right) \tag{16}$$

where $í_t$ is the vertically averaged turbulent exchange coefficient or eddy viscosity (Nezu and Rodi 1986),

$$v_t=\kappa\frac{1}{\xi}(1-\xi)u_*h_t \tag{17}$$

where κ is von Kármán constant (≈0.41); and

$$\xi=(z-z_{ch})/h_t \tag{18}$$

where h_t the whole depth of flow; z_{ch} is the elevation of local channel bed; u_* is the shear velocity.

Similarly, the stresses at the k-th interface are evaluated,

$$\sigma_x = 2\rho\nu_t \frac{\partial u_k}{\partial x} \tag{19}$$

$$\sigma_z = 2\rho\nu_t \left(\frac{\partial w}{\partial z}\right)_k = 2\rho\nu_t \frac{(w_{c,k-1} - w_{c,k})}{(h_{k-1} + h_k)/2} \tag{20}$$

$$\tau_{xz} = \tau_{zx} = \rho\nu_t \left(\frac{\partial u}{\partial z} + \frac{\partial w}{\partial x}\right)_k = \rho\nu_t \left(\frac{u_{c,k-1} - u_{c,k}}{(h_{k-1} + h_k)/2} + \frac{\partial w_k}{\partial x}\right) \tag{21}$$

For open channel flows, the assumption of pure shear stress applies to the channel bed (Steffler and Jin 1993). Then at channel bed, Eqs. (12 b) and (13b) reduce to,

$$F_{xb} = \tau_b;\ F_{zb} = \tau_b \frac{\partial z_{ch}}{\partial x} \tag{22a, b}$$

and the bed shear stress, τ_b, can be evaluated using Chezy formula,

$$\tau_b = \frac{\rho u_t (u_t^2 + w_t^2)^{1/2}}{C_*^2} \tag{23}$$

where u_t and w_t are the depth-averaged horizontal and vertical velocities over the total water depth; and C_* is the non-dimensional Chezy coefficient.

NUMERICAL SCHEME

EQUATIONS CLOSURE

In this paper, the flow is divided implicitly. Both the layer thickness and interface elevation are unknown. However, the elevation of each layer interface can then be located after the determination of layer thickness,

$$z_s = z_b + h \tag{24}$$

where z_b is known as the elevation of the n-th interface. Therefore, only the layer thickness is independent.

There are (n+1) unknown vertical velocities, w_k, at the layer interfaces. They correspond to the (n+1) interface equations, i.e., Eq. (1).

We placed the pressure at the (n+1) interfaces, and the pressure at the free surface is known as zero. Therefore there are only n unknown parameters for pressures. They correspond to the n vertical momentum equation, i.e., Eq (11).

The nodal points for horizontal velocity are located at both the layers' mid-thickness points and the interfaces, totally (2n+1) points. They correspond to the horizontal momentum and moment equations. However, there are only 2n such equations. To make them closure, we can simply assume that the horizontal velocity profile for the first layer is straight line. Then there are only 2n independent horizontal variables being consistent with the equations.

According to the characteristics of these unknowns and the equation forms, all of them can be categorized into two groups. The first group of the unknown variables includes the layer thickness h and horizontal velocity variables u_0 and u_1. The second group constitutes the parameters for vertical velocities, w_k, and pressure, p_b.

These unknown variables can be solved using different methods, such as finite element method, or finite difference method. Due to the rapid variation of channel bed, some oscillations of these variables will occur in the rapid varied segments. This oscillations can be dampened using artificial viscosity methods (Jameson et al. 1981; Chaudhry 1983).

SOLUTION STEPS

The steps are suggested as follows,

- Boundary conditions are imposed according to the basic principles and the specific cases;
- Predict the layer thickness and velocity with "predictor" for each layer from top to bottom;
- Evaluate the vertical velocity and pressure based on the predicted layer thickness and horizontal velocity for each layer interface from top to bottom;
- Correct the layer thickness and velocity with "corrector" or each layer from top to bottom;
- Evaluate the vertical velocity and pressure based on the predicted layer thickness and velocity for each layer interface from top to bottom;
- Dampen the oscillation of the dependent variables;
- Repeat from the second to the fifth steps till steady flows are approached.

APPLICATION

Sivakumaran et al (1983) performed a series of experiments for flows over symmetric and asymmetric bedforms. These experiments were in a 915 cm long, 65 cm high and 30 cm wide horizontal flume, which is made of a steel frame with glass windows on both vertical sides. The bed of 1.5cm thick plywood was elevated 10 cm above the base of the flume, to house the plastic tubes connecting the piezometer tapping along the centerline of the curved-bed model and piezometers. The inflow to the inlet box through a 15.24 cm diameter cast-iron pipe was controlled by a gate valve.

This paper selects the experimental flow over a symmetric bedform. The symmetric profile of the 120 cm is described by the normal distribution,

$$y = 20\exp[-\frac{1}{2}(\frac{1}{24}x)^2] \tag{25}$$

where x, y =horizontal and vertical coordinates in cm.

The leading edge of the profile was placed 366 cm downstream the inlet box. The upstream undisturbed depth was measured at 16 cm from the leading edge of the profile, and is used as an upstream boundary condition for the models. The symmetric profile was shaped according to a normal distribution and was 20 cm high and 120 cm long. The experiments only include the free surface profile and bed pressure, and experimental inflows are q =0.036 $m^3/s/m$ and q = 0.112 $m^3/s/m$.

The results are shown in Figures 3 and 4. For both cases, their surface profiles are simulated very well. Their bed pressure profiles are also well simulated.

Though the mathematical model provides vertical distribution information for velocities and pressure in addition to the profiles of the free surface and bed pressure, the comparison for velocity and pressure distribution are not performed due to the lack of experimental results.

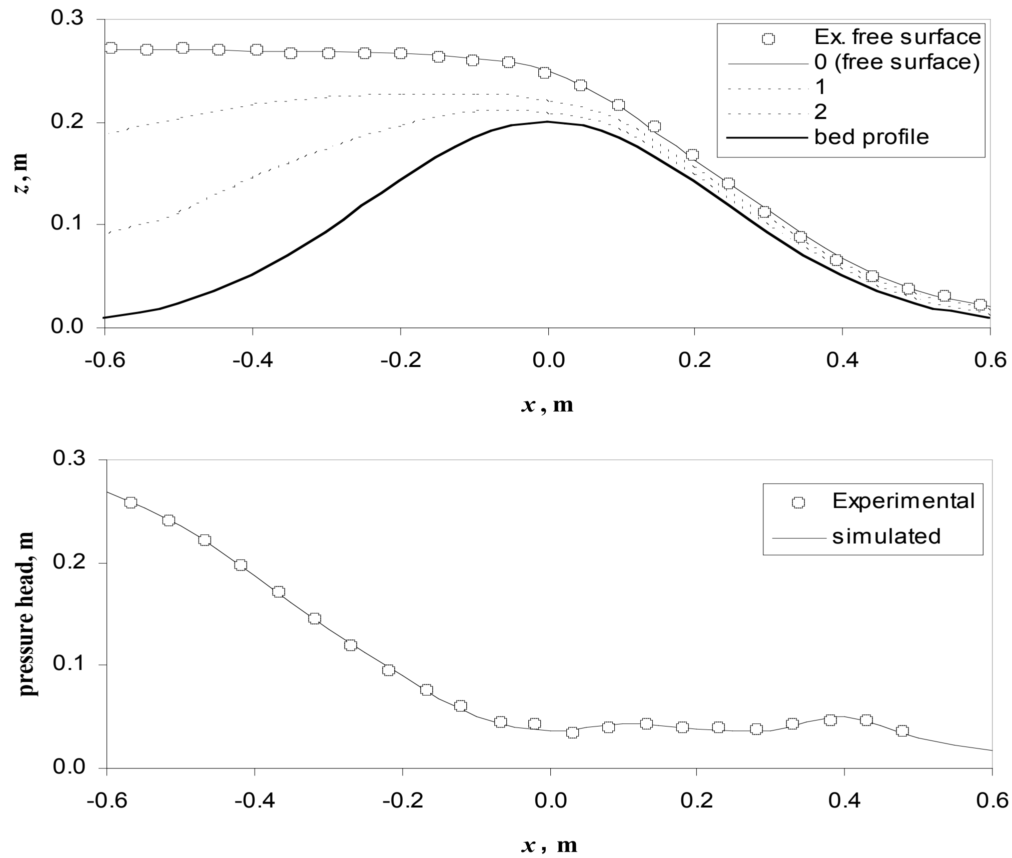

Figure 3: Flow over symmetric Bedform (q = 0.036 m^3/s/m)

(a) Free surface and intefaces (b) Bed Pressure

CONCLUSIONS

Comparing to the other methods, the multilayer models can supply much more vertical detail while limiting the added computation. In the models, the layer dividing interfaces can use explicit or implicit method; and the governing equations can become the basic depth-averaged equations.

In this paper, the layer dividing is carried out by implicit method, by which the governing equations are simplified; it could adjust to the flow conditions. The simulation is carried out in each layer, and it is repeated layer by layer, from the top to the bottom. The model is used in the simulation of flows of two different discharges over a symmetric bedform. It includes. The results demonstrated that the model can simulate the free surface profile, bed pressure profile well.

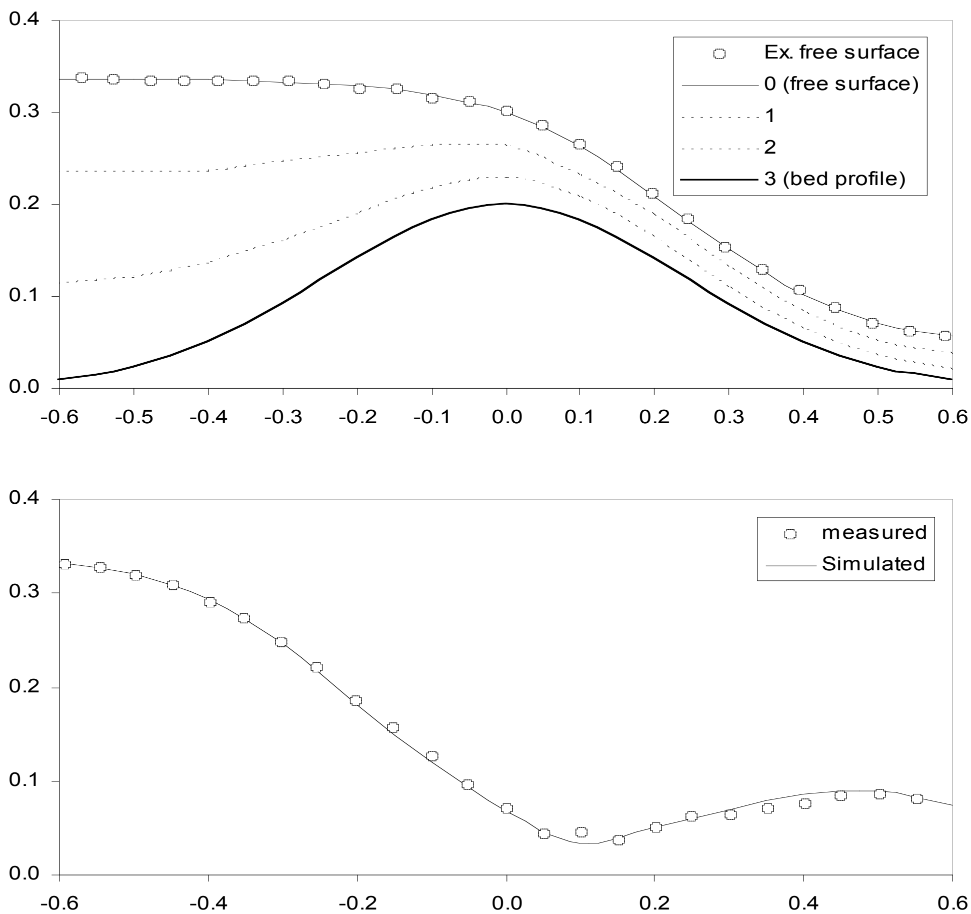

Figure 4: Flow over symmetric Bedform (q = 0.112 m^3/s/m)

(a) Free surface and intefaces (b) Bed Pressure

REFERENCES

Chaudhry, H. M. (1993). “Open-channel flows.” Prentice Hall, Englewood Clifts, NewJersey.

Chio, S. -U. (1998). "Layer-averaged modeling of two-dimensional turbidity currents with a dissipative Galerkin finite element method. part I: formulation and application example." *J. Hydr. Res.*, IAHR, 36(3), 339-363.

Dressler, R. F. (1978). "New nonlinear shallow flow equations with curvature." *J. Hydr. Res.*, IAHR, 16(3), 205-222.

Jameson, A., Schmidt, W. and Turkel, E. (1981). "Numerical solution of the euler equations by finite methods using Runge-Kutta time stepping schemes." *AIAA 14th Fluid and Plasma Dynamics Conference*, Palo Alto, California.

Lai, C. J. and Yen C. W. (1993). "Turbulence free surface flow simulation using a multilayer model." *Int. J. Nume. Meth. Fluids*, 16(11), 1007-1025.

Lynett, P. J. and Liu, P. L. F. (2004). "Linear analysis of the multi-layer model." *Coastal Engrg.*, 51(5-6), 439-454.

Matthew, G. D. (1991). "High order, one-dimensional equations of potential flow in open channels." *Proc. Instn. Civ. Engrs: Water, Mart. Engy.*, Part 2, 91, 187-201.

Montes, J. S. (1994). "Potential-flow solution to 2D transition from mild to steep slope." *J. Hyd. Engrg.*, ASCE, 120(5), 601-621.

Nezu, I. and Rodi, W. (1986). "Open–channel flow measurements with laser Droppler anemometer." *J. Hydr. Engrg.*, ASCE, 112(5), 335-355.

Reggio, M., Hess, A. and Ilinca, K. (2002). "3-D multiple-level simulation of free surface flows." *J. Hydr. Res.*, IAHR, 40(4), 413-423.

Sivakumaran, N. S., Tingsanchali, T. and Hosking, R.J. (1983). "Steady shallow flow over curved beds." *Journal of fluid mechanics*, 128, 469-487.

Steffler, P. M. and Jin, Y. (1993). "Depth-averaged and moment equations for moderately shallow free surface flow." *J. Hydr. Res.*, IAHR, 31(1), 5-17.

Versteeg H. K. and Malalasekera W. (1995). *An introduction to computational fluid dynamics-the finite volume method*. Pearson Prentice Hall, Essex, England.

Wai, W. H., Lu, Q. and Li, Y. S. (1996). "Multi-layer modeling of three-dimensional hydrodynamic transport processes." *J. Hydr. Res.*, IAHR, 34(5), 677-693.

Xia, C. and Jin, Y. (2005*a*). "Modeling 1-D flow with multilayered moment equations." Proceedings of the 17th Canadian Hydrotechnical Conference (CDROM), Edmonton, Canada

Xia, C. and Jin, Y. (2005*b*). "Multilayer averaged and moment equations for open-dimensional open channel flows." paper accepted for publication, *J. Hydr. Engrg.*, ASCE

Zarrati, A. R. and Jin, Y. C. (2004). "Development of a generalized Multi-Layer Model for 3D simulation of free surface flows." *Int. J. Nume. Meth. Fluids*, 46, 1049-1067.